

---

# Direct Numerical Simulation of fractal-generated turbulence

S. Laizet<sup>1</sup> and J.C. Vassilicos<sup>1</sup>

Turbulence, Mixing and Flow Control Group,  
Department of Aeronautics and Institute for Mathematical Sciences,  
Imperial College London,  
London SW7 2AZ, United Kingdom [s.laizet@imperial.ac.uk](mailto:s.laizet@imperial.ac.uk)

**Summary.** The flow obtained behind a fractal square grid is studied by means of direct numerical simulation. An innovative approach which combines high order schemes, Immersed boundary method and a dual domain decomposition method is used to take into account the multiscale nature of the grid and the resulting flow.

## 1 Introduction

Recently at Imperial College London, experiments of turbulence generated by fractal grids (see Fig. 1) placed at the entrance of a wind tunnel have shown some unprecedented properties. For example, a fractal square grid can generate a far downstream decaying homogeneous isotropic turbulence with broad power law (approximately  $-5/3$ ) energy spectra but laminar-like dissipation [1], [7]. Although the wind tunnel measurements have provided invaluable time-resolved informations on the unique properties of multiscale generated turbulent flows, understanding the spatial structure of these flows is also necessary to discover the origins of these properties. In this paper, with the help of the new generation of parallel-architecture platforms, it is suggested that Direct Numerical Simulation (DNS) can provide the spatio-temporal information of the flow and be an important complement to advanced experimental techniques, despite the very large simulations required. As a preliminary study, a DNS of the turbulent flow generated by one of the fractal square grids used for the experimental measurements is presented here.

## 2 Numerical methods

A numerical code fully based on sixth-order compact finite-difference schemes and a Cartesian mesh is used to solve the incompressible Navier-Stokes equations. The incompressibility condition is ensured via a fractional step method introducing a Poisson equation for the pressure. An original characteristic of the present code, called **Incompact3d**, is that this equation is directly solved in the framework of the modified spectral formalism. More precisely, our Poisson solver is only based on

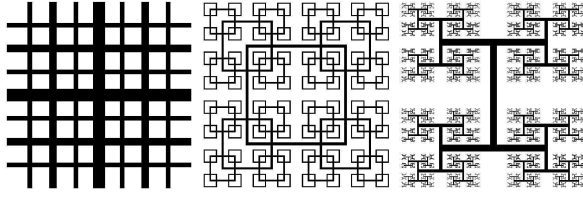


**Fig. 1.** Scaled diagrams of a fractal cross grid (left), a fractal square grid (middle) and a fractal I grid (right).

3D Fast Fourier Transforms (FFT3D) despite the use of inflow/outflow boundary conditions. This very direct solving technique is obviously possible for periodic and free-slip boundary conditions, but also when Dirichlet conditions for the velocity are combined with homogeneous Neumann conditions for the pressure (see for instance [8] for the basic principles of the spectral solution of a Poisson equation based on cosine expansions). Note that the Poisson equation's solution cost is less than 10% of the overall computational expense. Concerning the pressure mesh, we follow here conclusions previously reached by [2], [3] and use a staggered pressure mesh in order to avoid spurious pressure oscillations particularly when the code is combined with an immersed boundary method. More details about the present computational methodology can be found in [3].

The fractal grid is modelled using an immersed boundary technique where the specific direct forcing method of [6] is employed. The basic principle is to adapt the forcing which replaces and models the effects of the immersed solid grid in a way which yields the no-slip condition at the boundary between grid and fluid.

The parallel version of **Incompact3d** (with MPI implementation for running on massive parallel platform) is used here because of the multiscale nature of the fractal grid. The code's dual domain decomposition strategy offers two major advantages: parallelisation is possible without reducing the order of our schemes, and scalability is excellent (up to more than 1000 processors) because, even though our schemes are implicit in space, there is no data communication (overlapping) at the boundaries of each subdomain [4].

### 3 The fractal square grid

For this preliminary numerical study, only one family of fractal grids is considered, which consists of different sized squares with 4 rectangular bars (see Fig. 1, middle). This fractal grid is completely characterised by

- the number of fractal iterations  $N = 4$
- the bar lengths  $L_j = R_L^j L_0$  and thicknesses  $t_j = R_t^j t_0$  (in the plane of the grid, normal to the mean flow) at iteration  $j$ ,  $j = 0, \dots, N - 1$  ( $0.19M_{eff}$  for the thickness in the direction of the mean flow, see below for  $M_{eff}$ ).  $R_L = 1/2$ ,  $R_t = 0.584$ ,  $L_0 = 0.5L_y$ ,  $L_3 = 0.125L_0$ ,  $t_0 = 0.4 M_{eff}$  and  $t_3 = 0.08M_{eff}$  for the grid considered here.
- the number  $B^j$  of patterns at iteration  $j$  ( $B = 4$ ).

By definition,  $L_0 = L_{max}$ ,  $L_{N-1} = L_{min}$ ,  $t_0 = t_{max}$  and  $t_{N-1} = t_{min}$ . The blockage ratio  $\sigma$  of this grid is the ratio of its total area to the area  $T^2$  of the tunnel's cross section ( $T = L_y = L_z$ ) and is equal to 25%. It is also of interest to define the thickness ratio  $t_r = t_{max}/t_{min} = 5$ . Unlike classical grids, the grid considered here does not have a well-defined mesh size. [1] introduced an effective mesh size for multiscale grids  $M_{eff} = \frac{4T^2}{P}\sqrt{1-\sigma}$  where  $P$  is the grid's perimeter length in the  $(y-z)$  plane. Note that the fractality of the grid influences  $M_{eff}$  via its perimeter  $P$  which can be extremely long in spite of being constrained to fit within the area  $T^2$ . For the grid considered here,  $M_{eff} = 26.5mm$ .

The governing equations are directly solved in a computational domain  $L_x \times L_y \times L_z = 36.5M_{eff} \times 18.25M_{eff} \times 18.25M_{eff}$  discretized on a Cartesian mesh of  $n_x \times n_y \times n_z = 2305 \times 1152 \times 1152$  mesh nodes. Inflow/outflow, and periodic boundary conditions are used in the x direction and y-z directions respectively. Based on a preliminary study [5], the streamwise position of the grid ( $5t_{min}$  from the inflow boundary of the computational domain) has been carefully chosen to avoid any spurious interactions between the modelling of the grid and the inflow boundary condition. Note that the parameters of the targeted grid correspond to one of the grids used in the laboratory experiments of [1] (Fig. 32b in [1]). Indeed, one of the imperatives of this preliminary numerical study is to be as close as possible to the experimental set-up of [1]. However, the DNS has one significant difference compared to the experiments: the Reynolds number  $Re_{M_{eff}} = \frac{U_\infty M_{eff}}{\nu}$  is reduced from 20800 to 3785. Consequently, only a qualitative agreement with experiments can be expected.

Due to the multiscale nature of the grid, the simulation requires state-of-the art top-end parallel computing and therefore the number of mesh nodes is of crucial importance. A preliminary study [5] has shown that five mesh nodes is enough to discretize the smallest thickness  $t_{min}$  of a fractal grid for the Reynolds number considered here.

## 4 Results

One of the most interesting experimental results is that, for the fractal square grids, two regions exist downstream from the grid: a turbulence production region where the turbulence intensity continuously increases till it reaches a peak, and a turbulence dissipation region where the turbulence is approximately homogeneous and isotropic [1]. Remarkably, the integral and Taylor length-scales remain constant during decay far downstream of fractal square grids (as opposed to regular grids where they markedly increase). For our simulation, we can observe a considerably complex turbulent flow due to the multiscale nature of the grid. An illustration of the flow is presented in figs. 2 and 3 through instantaneous streamwise velocity visualisations. These visualisations clearly suggest that there are interactions between the different wakes, at different scales and at different locations. The production of turbulence observed in [1] could result from these sequential interactions between wakes, from small-scale ones all the way up to the large-scale ones. It should be noted also that the influence of the shape of the fractal grid remains important far from the grid and strongly influences the flow as shown in fig. 3. Indeed, at the end of the computational domain, the turbulence reached is still far from isotropic even if  $u'/v'$  and

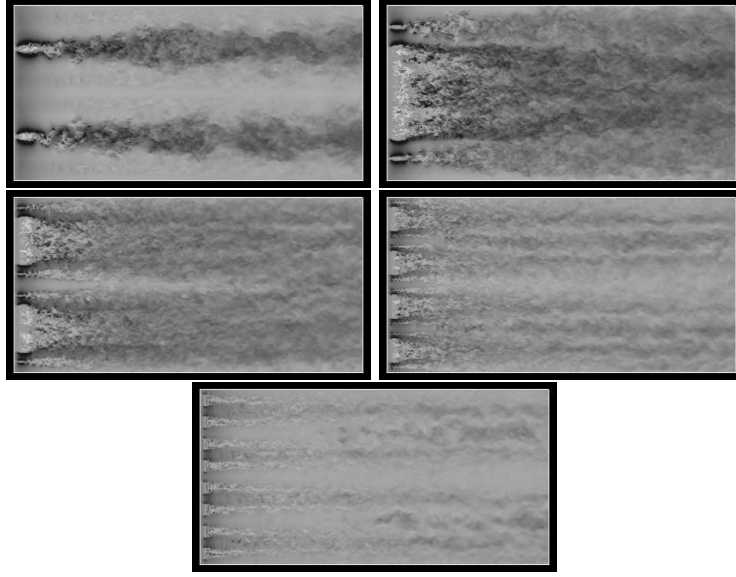


**Fig. 2.** Instantaneous streamwise velocity in the  $(x - z)$  plane, for  $y/T = 0, 0.25, 0.125, 0.0625$  and  $0.03125$ .

$u'/w'$  are roughly the same (see fig. 4). Unfortunately the big wakes generated by the bigger square only start to interact at the end of the computational domain. For this reason, it was not possible to observe the peak in turbulence intensity on the centreline ( $y/T = z/T = 0$ ) and a subsequent decay as in the experimental measurements [1].

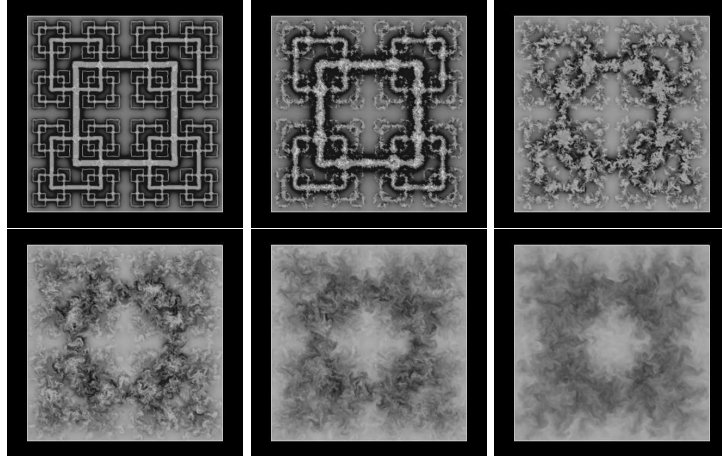


**Fig. 3.** Instantaneous streamwise velocity in the  $(y - z)$  plane for  $x/M_{eff} = 0.5, 1.5625, 3.125, 6.25, 12.5$  and  $25$ .

These initial conclusions can be confirmed with some turbulence intensity statistics presented in fig. 4. We can observe a production of turbulence for  $u'$  at different locations in the vertical direction behind the grid. It should be noted that this production of turbulence seems to be smaller for  $v'$  and  $w'$ . Our simulation suggests that, it is possible for a new production region to exist downstream of the first one (see for instance, the streamwise profile of  $u'$  for  $y/T = 0.125$  on fig. 4, top right). These two peaks were clearly identified in a movie of the numerically simulated streamwise velocity and the second peak seems to result from the interaction with the largest bar's wake which occurs at about  $x/M_{eff} = 27$ . This represents a clear prediction for future experimental measurements to be made at different lateral locations.

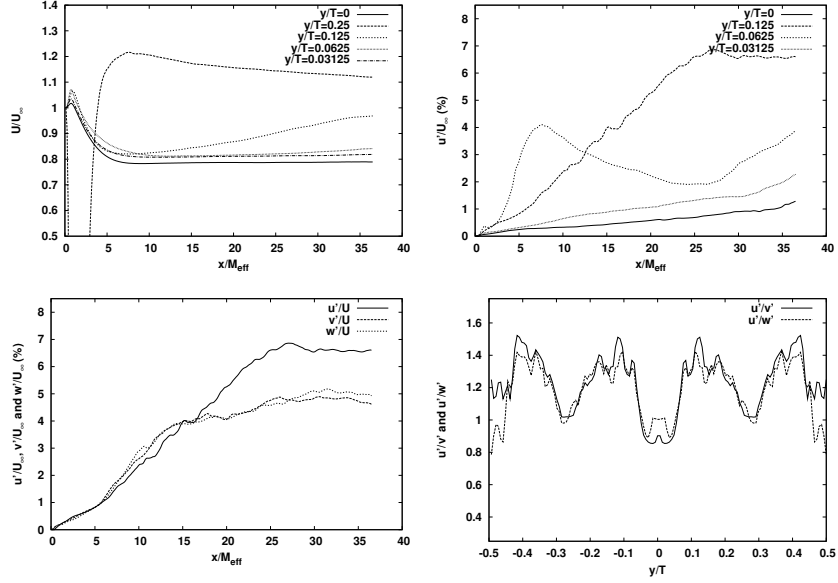


**Fig. 4.** Streamwise evolution of the mean velocity for different  $y/T$  and for  $z/T = 0$  (Top, left); streamwise evolution of  $u' / U_{\infty}$  for different  $y/T$  and for  $z/T = 0$  (Top, right); streamwise evolution of turbulence intensities for  $y/T = 0.125$  and for  $z/T = 0$  (bottom, left); Large-scale isotropy indicators at  $x/M_{eff} = 31$  (bottom, right).

Due to the limited size of the computational domain in the streamwise direction, it is not possible to observe the decay region which follows the production region, especially on the centreline. Note also that the location of the peak of turbulence may have a dependence on the Reynolds number as this peak was found to be much closer in the experimental results (where the Reynolds number was more or less five times bigger). The experimental results suggest that, by increasing the thickness of the biggest square (increasing  $t_r$ ) it should be possible to observe a peak of turbulence much closer to the grid which will be useful for future simulations.

## 5 Conclusion

In spite of the difference in Reynolds number, the present DNS results are very encouraging. A long post-processing and more comparisons with the experimental results are now required in order to better understand the properties and dynamics of this new turbulent flow. It will also be necessary to increase the computational domain in the streamwise direction in order to study the turbulence in the decay region. A large range of  $t_r$  will also need to be investigated. Unfortunately, it will not be possible to increase the Reynolds number due to computational considerations and future comparisons between experiments and simulations will have to take this into account. Indeed, because of the multi-scale nature of the grid, already more than five billions mesh nodes were needed for this DNS on one of the state-of-the-art parallel-architecture platform.

## 6 Acknowledgments

We acknowledge the EPSRC grant EP/F051468 and the UK Turbulence consortium for the CPU time made available to us on HECToR without which this paper would not have been possible. The authors are grateful to Roderick Johnstone for help with the parallel version of **Incompact3d**. We also thank Eric Lamballais for very useful discussions and acknowledge support from EPSRC Research grant EP/E00847X.

## References

1. D. Hurst and J. C. Vassilicos. Scalings and decay of fractal-generated turbulence. *Phys. Fluids*, **19**:035103, 2007.
2. S. Laizet and E. Lamballais. Compact schemes for the DNS of incompressible flows: in what context is the quasi-spectral accuracy really useful? In *Proc. IV Escola de Primavera de Transição e Turbulência*, Porto Alegre, RS, Brazil, 2004.
3. S. Laizet and E. Lamballais. High-order compact schemes for incompressible flows: a simple and efficient method with the quasi-spectral accuracy. *J. Comp. Phys.*, Submitted, 2008.
4. S. Laizet, E. Lamballais, and J.C. Vassilicos. A numerical strategy to combine high-order schemes, complex geometry and massively parallel computing for the dns of fractal generated turbulence. *Computers and Fluids*, Submitted, 2008.
5. S. Laizet and J.C. Vassilicos. Multiscale generation of turbulence. *Journal of Multiscale Modelling*, 1:177–196, 2009.
6. P. Parnaudeau, E. Lamballais, D. Heitz, and J. H. Silvestrini. Combination of the immersed boundary method with compact schemes for DNS of flows in complex geometry. In *Proc. DLES-5*, Munich, 2003.
7. R. E. Seoud and J. C. Vassilicos. Dissipation and decay of fractal-generated turbulence. *Phys. Fluids*, **19**:105108, 2007.
8. R. B. Wilhelmson and J. H. Ericksen. Direct solutions for Poisson’s equation in three dimensions. *J. Comput. Phys.*, **25**:319–331, 1977.